Toward an Integral Interpretation of the Optical Steady-State Spectra of the FMO-Complex of *Prosthecochloris aestuarii*. 1. An Investigation with Linear-Dichroic Absorbance-Detected Magnetic Resonance

R. J. W. Louwe, J. Vrieze, T. J. Aartsma, and A. J. Hoff*

Department of Biophysics, Huygens Laboratory, Leiden University, P.O. Box 9504, 2300 RA Leiden, The Netherlands

Received: July 8, 1997[⊗]

In this paper we present results of (linear-dichroic) absorbance-detected magnetic resonance experiments on the FMO-complex of *Prosthecochloris aestuarii* at 1.2 K. We have used these results as additional criteria for testing exciton simulations of the optical spectra of this complex. We find that the photo-excited triplet state is localized on a single bacteriochlorophyll *a* chromophore of the complex associated with a $S_1 \leftarrow S_0$ transition at ∼825 nm in the Q_Y-absorption region (790−830 nm). The orientations of several optical transition moments in the Q_Y-absorption band relative to the triplet *x*- and *y*-axes of the triplet-carrying molecule have been determined. Comparison of the triplet-minus-singlet absorbance-difference spectra with simulations using parameter sets from the literature shows significant discrepancies, which can be traced to an overestimation of the dipolar interactions between the individual bacteriochlorophyll *a* molecules. Exciton simulations based on considerably lower dipolar interactions, presented in an accompanying paper, show considerable improvement of the fits to the relevant optical steady-state spectra.

1. Introduction

The bacteriochlorophyll *a*-protein (FMO) complex of green sulfur bacteria is one of the best characterized pigment-protein complexes in photosynthesis. Due to its solubillity in water, this complex is readily isolated and crystals suitable for X-ray crystallography are relatively easy to obtain.[1] Therefore, this pigment-protein complex was the first of which the structure was determined (see, for example, refs 2 and 3). More recently, near-atomic resolution of the structure was obtained by refinement of the X-ray data.[4] The complex consists of three identical subunits organized in C_3 symmetry, and each subunit contains seven bacteriochlorophyll (BChl) molecules. The shortest center-to-center distance between two BChls within one subunit is 12 Å, while the shortest distance between two BChls belonging to different subunits is 24 Å.

At low temperatures the absorption spectrum of the FMO-complex shows significant structure, in both the Q_Y (790−830 nm) and the Q_X (590−630 nm) absorption region.[5] The linear dichroism (LD)[6−8] and circular dichroism (CD) spectra[9−11] at low temperatures show similar spectral structure. FMO-complexes isolated from different species exhibit small variations in peak positions and amplitudes of the absorption bands.[12]

A simultaneous simulation of the low-temperature absorption- and CD-spectrum of the FMO-complex has been presented by Pearlstein et al.[13,14] using the exciton formalism. Results of transient absorption[15−17] and hole-burning experiments have been explained with the results of Pearlstein at al., notwithstanding significant discrepancies between the Pearlstein model and the experimental results. For example, Gülen[19] noted that it was not possible to obtain reasonable simulations of the triplet-minus-singlet (T−S) and LD-spectra using the parameter sets presented in refs 13 and 14. She presented an alternative set of parameters which improved the fit of the exciton simulations to the LD-absorption and flash-induced T−S spectrum[8] considerably, but the CD spectrum could still not be reproduced.

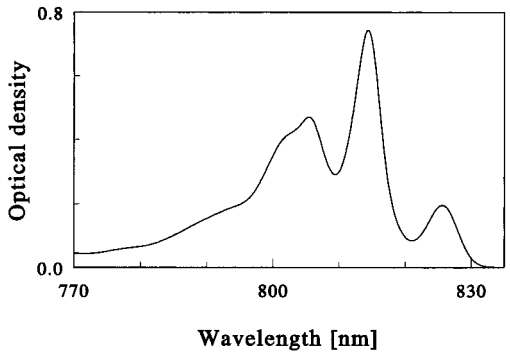

Figure 1. Absorption spectrum of the FMO-complex at 1.2 K.

The T−S spectra of pigment-protein complexes are usually interpreted in terms of changes in the absorption spectrum due to the loss of oscillator strength of the triplet-carrying pigment, and consequently a redistribution of the oscillator strengths of other pigments because of the reduction in dipolar interactions. Exciton simulations based on such an interpretation are not always successful, however, despite the detailed structural information that is available in a number of cases. For example, for reaction center complexes, it has been shown that the bandshifts and polarizations of various transitions as observed in the T−S spectra cannot be explained in terms of an exciton model.[20]

Here we report on absorbance-detected magnetic resonance (ADMR) experiments in zero-magnetic field on the FMO-complex of *Prosthecochloris (P.) aestuarii*. ADMR is a double-resonance technique, in which optical absorbance differences are monitored that result from microwave-induced transitions between the spin sublevels of the triplet state. The energy differences between the spin-sublevels are characterized by the zero-field splitting (zfs-) parameters, *D* and *E* (Figure 2, inset). The T−S spectra obtained with this technique provide information about the interaction between the chromophores. Due to the selection of a particular frequency within the inhomogeneously broadened microwave-induced absorbance difference

* Author to whom correspondence should be addressed.
⊗ Abstract published in *Advance ACS Abstracts,* November 15, 1997.

S1089-5647(97)02215-3 CCC: $14.00

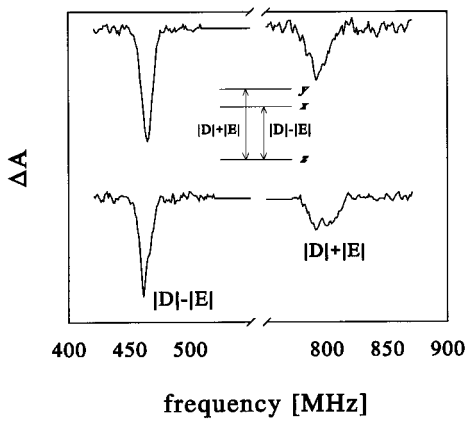

Figure 2. The ODMR spectra at the $|D| - |E|$ (left) and $|D| + |E|$ (right) transitions. The detection wavelength is 827 nm, in the presence (upper spectra) and absence (lower spectra) of dithionite.

band, enhanced optical resolution is obtained as compared to flash-induced absorbance difference spectroscopy.

With LD-ADMR, the orientations of the optical transition moments in the Q_Y-region (790−830 nm) with respect to the triplet *x*- and *y*-axes of the triplet-carrying chromophore can be determined.[21,22] With this technique, the difference is measured between the T−S spectra obtained with light polarized parallel and perpendicular to a macroscopic orientation axis, respectively. The macroscopic orientation axis is the polarization direction of the microwave magnetic field at a resonance frequency within the $|D| - |E|$ (or $|D| + |E|$) transition, so that only those molecules which have their microwave transition moment *y* (or *x*) parallel to this direction contribute to the absorbance difference ΔA. Bands that are not resolved in the T−S spectrum and that have a different orientation with respect to the triplet axis, may be resolved in the LD-(T−S) spectra. The observed anisotropy R_i is related to the orientation of specific optical transition moments within the triplet axis frame $\{\vec{x}_T\vec{y}_T\vec{z}_T\}$ by:[22,23]

$$R_i = \frac{\text{LD-(T−S)}}{\text{T−S}} = \frac{\Delta A_{\parallel} - \Delta A_{\perp}}{\Delta A_{\parallel} + \Delta A_{\perp}} = \frac{(3\cos^2\alpha_i - 1)}{(3\cos^2\alpha_i + 1)} \qquad i = x, y, z \quad (1)$$

where α_i is the angle between the triplet *i*-axis and the optical transition moment of a specific band in the ΔA spectrum.

Although the three microwave transitions are mutually perpendicular ($\cos^2\alpha_x + \cos^2\alpha_y + \cos^2\alpha_z = 1$), the values for R_i obtained for two different microwave transitions do not uniquely define the orientation of the optical transition dipole moment in the $\{\vec{x}_T\vec{y}_T\vec{z}_T\}$ axes frame of the triplet dipolar tensor. Due to the dependence of R_i on $\cos^2\alpha_i$, measurement of R_x and R_y yields eight possibilities for the orientation of an optical transition moment in the triplet axes frame. This leads to four possible relative orientations (within a quadrant of 90°) of two different optical transition moments. When both optical transition moments are polarized in the triplet $\vec{x}_T\vec{y}_T\vec{z}_T$-plane, the number of relative orientations reduces to two.

In this paper we will present a comparison of the experimental and simulated T−S and LD-(T−S) spectra using the previously published parameter sets for exciton simulations mentioned above and assess the validity of these parameter sets.

2. Experimental Section

The FMO-complex was isolated from *P. aestuarii* by a procedure similar to that described in ref 24. The protein was dissolved in a 50 mM Tris/HCl buffer (pH = 7.8) containing 750 mM NaCl. Glycerol (66 % v/v) was added to obtain an optically clear glass at low temperature. The optical density was ∼0.35 at 810 nm at room temperature in a flat (path length 1 mm) plexiglass cuvette. All experiments were performed at ∼1.2 K in a liquid He-bath cryostat. The ADMR set-up was basically the same as described in ref 25. Continuous white light from a tungsten−iodine lamp was used for excitation and for probing the transmittance. The light transmitted by the sample was passed through a monochromator (Jobin-Yvon, 1200 lines/mm, blaze 750 nm) with the optical resolution set at 3 nm, and detected by a Peltier-cooled photodiode (RCA 30842). The sample cuvette was placed in a tunable split-ring cavity ($Q \approx 100$) connected to a microwave source, such that the direction of the magnetic field component of the microwave radiation was perpendicular to the path of the light beam. The change in transmitted light intensity ΔI, induced at a frequency of 312 HZ by amplitude modulation of the microwaves, was measured by phase-sensitive detection using a lock-in amplifier. The absorbance-difference (ΔA) signal is to a good approximation proportional to the ratio of the change in transmitted light intensity ΔI and the transmitted light intensity *I*, which were recorded simultaneously.

For LD-ADMR experiments, a photoelastic modulator (PEM) and a Glan−Thompson polarizer was placed in the light path between the sample and the monochromator for analyzing the change in transmittance of the sample with light polarized either parallel or perpendicular to the polarization of the microwave magnetic field. This $\Delta(\Delta I)$ signal was recorded using two lock-in amplifiers in series. The first one was locked at twice the modulation frequency of the PEM (100 kHz), while the second one was locked at the modulation frequency of the microwaves.[21]

To avoid saturation effects (similar to those in photoselection measurements) in the determination of R_i, it is necessary to extrapolate the T−S and LD-(T−S) signals to zero microwave power. Therefore, R_i of a particular absorbance band was calculated from the slope of the plot of the LD-(T−S) against the T−S amplitudes, which were extrapolated to zero microwave power. To avoid experimental errors in the T−S signal due to the non-sinusoidal modulation of the PEM,[26] the determination of R_i was performed without the PEM. In this case the magnitude of the LD-(T−S) signal is given by the difference of the T−S signals measured with vertical and horizontal orientation of the polarizer, respectively.[27]

Exciton calculations were performed as described in ref 28. The dipolar interactions between the chromophores, calculated in the point−monopole approximation, were taken from ref 13. The X-ray data (denoted as model 5R,[4]) were obtained from the Brookhaven National Data Bank.

3. Results

3.1. The FMO-Complex in the Absence of Dithionite. The low-temperature (1.2 K) absorption spectrum of the FMO-complex (Figure 1) in the Q_Y region is virtually identical to that reported previously[5,12] and consists of several resolved bands, centered at 825, 814, and 805 nm, a shoulder at 800 nm, and a relatively broad band, centered at ∼795 nm.

The ADMR spectra of the FMO-complex were determined by monitoring the absorption changes at 827 nm in the long-wavelength absorption band as a function of the microwave frequency. The resonance frequencies at ∼465 and ∼795 MHz correspond to the $|D| - |E|$ and $|D| + |E|$ transitions between the triplet sublevels and are similar to those of monomeric BChl *a*.[29,30] The zfs-parameters $|D|$ and $|E|$ are identical to those reported earlier[31] for the FMO-complex.

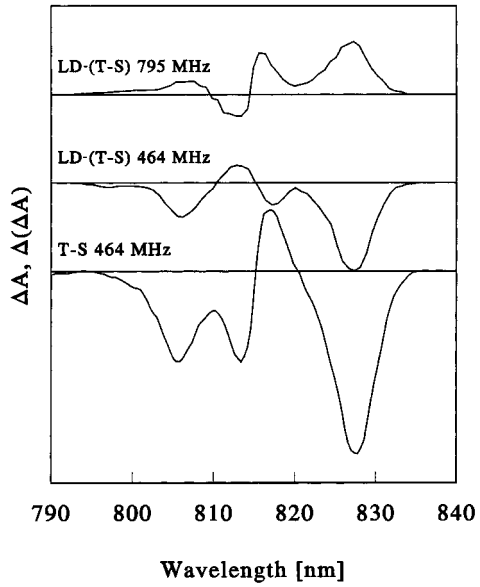

Figure 3. The T−S and LD-(T−S) spectra recorded at the microwave frequencies 464 and 795 MHz. The LD-(T−S) spectra are normalized to the T−S spectra via the value for R_i of the long-wavelength band.

The microwave transitions in Figure 2 have line widths of 10 and 14 MHz for the $|D| - |E|$ and $|D| + |E|$ transitions, respectively. A larger width for the ($|D| + |E|$) transition is commonly observed for BChls *in vivo* and *in vitro*. In contrast to what is observed for other pigment−protein complexes, the microwave resonance frequencies were independent of the detection wavelength within the experimental accuracy of 1 MHz. This, as well as the narrow line widths of the resonance bands, indicate that the preparation was highly homogeneous. Moreover, the environment of the triplet-carrying molecule in the BChl *a* complex appears to be much less heterogeneous than that in other pigment−protein complexes, such as reaction center complexes. In comparison, the line widths of the $|D| - |E|$ and $|D| + |E|$ transitions in chromatophores of *Rb. sphaeroides* R26 are 13 and at least 14 MHz, respectively, while for isolated RCs of the same species, these numbers are about 30 and 40 MHz.[32−34] In the latter case the substantial broadening of the microwave transitions is related to a significant heterogeneity of the sample, presumably incurred by the isolation procedure.

The microwave-induced T−S absorbance-difference spectrum of the FMO-complex recorded at 464 MHz ($|D| - |E|$ transition) is shown in Figure 3. The T−S spectrum closely resembles the flash-induced T−S spectrum[8] and is characterized by a relatively large negative band at the long-wavelength side of the spectrum (827 nm), a combination of a positive and a negative band typical of a band shift around 815 nm, and a smaller bleaching centered at ∼805 nm. The T−S spectrum associated with the $|D| + |E|$ transition had a similar shape (not shown), with a somewhat smaller amplitude of the negative 805 nm band. The maximum of the 827 nm band in the T−S spectrum is shifted ∼2 nm with respect to that of the 825 nm band of the absorption spectrum. This might be related to the same phenomenon observed in (bacterio-)chlorophyll in organic solvents[29] (see section Discussion). We verified with transient ADMR experiments using short microwave pulses that the negative sign of the ADMR signal at 827 nm corresponds to an increase in ground-state absorption upon microwave irradiation (data not shown).

The value for R_i of the long-wavelength band in the T−S spectrum was determined as described in the experimental section and the result of this procedure is shown in Figure 4.

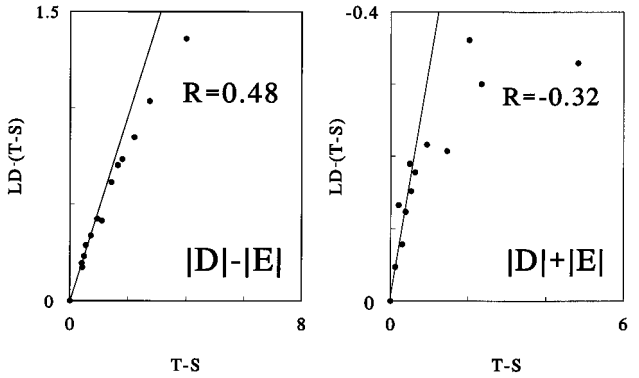

Figure 4. The LD-(T−S) amplitude plotted against the T−S amplitude. The microwave frequency was set at 465 MHz ($|D| - |E|$) and 795 MHz ($|D| + |E|$), respectively.

The data in Figure 4 was measured at 827 nm for both the $|D| - |E|$ as well as the $|D| + |E|$ transition at various microwave powers. At the $|D| + |E|$ transition $R_x = -0.32 \pm 0.02$ and at the $|D| - |E|$ transition, $R_y = 0.48 \pm 0.02$. These values correspond to $\alpha_x = 80-90°$ and $\alpha_y = 0-10°$ for the angle between the optical 827 nm transition moment and the triplet *x*- and *y*-axis of the triplet-carrying molecule, respectively. We present these angles as a range, rather than a fixed value with an error margin, because of the nonlinear dependence of α on R. We verified that R_i is constant over the entire 827 nm band, which indicates that there are no unresolved, overlapping bands in this wavelength region. We note that R_x and R_y are very similar to what has been found for BChl *a* in a range of organic solvents.[29]

The LD-(T−S) spectra were recorded at 464 and 795 MHz, simultaneously with the corresponding T−S spectra, at fixed microwave power (Figure 3). The LD-(T−S) spectra both exhibit a remarkable similarity to the T−S spectrum, i.e., a change in absorption at ∼827 nm, two bands typical of a bandshift around ∼815 nm, and another change in absorption at ∼805 nm. At first sight, there is no indication of the presence of other unresolved bands in the spectra. To obtain a more quantitative analysis, the LD-(T−S) spectra in Figure 3 were first scaled to the T−S spectrum at the maximum of the long-wavelength band using the value for R_i of these bands. Here after, the T−S and both LD-(T−S) spectra were fitted to a sum of Gaussian bands using global analysis. This result is shown in Figure 5 and Table 1. It is possible to fit all spectra within the instrumental error using a minimum set of five Gaussians with an equal width of 80 cm^{-1} fwhm. One band is needed to account for the bleaching at 827 nm, two bands with opposite amplitude for the bandshift around 815 nm, one band for the bleaching at 805 nm, and a minor band at 800 nm. Upon comparison of the sign and amplitudes of the bands in the T−S spectrum with those of the corresponding bands in the LD-(T−S) spectra, the orientation of the corresponding transition dipoles with respect to the triplet *x*- and *y*-axes is determined using eq 1. The angles between the transition dipole of the 814/815 nm band and the triplet *x*- and *y*-axes are ∼18° and ∼76°, respectively, approximately perpendicular to the 827 nm transition dipole moment. We observe no significant contribution of a bleaching around this wavelength, nor do we observe a change in polarization. Apparently, the change of sign of ΔA around 815 nm can be described by a pure bandshift.

The transition absorbing at 805 nm is found to be oriented more or less parallel to the 827 nm transition moment. Since the angles between the optical transition dipole moment and the triplet *x*- and *y*-axes add up to approximately 90° for every transition, all the Q_Y-transitions appear to be polarized parallel

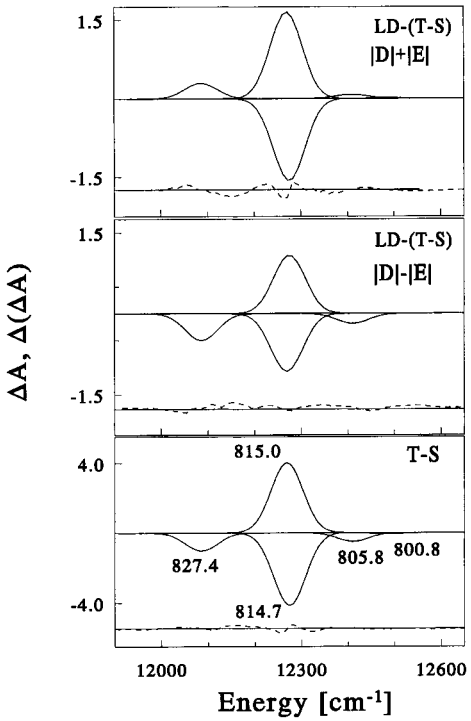

Figure 5. Gaussian bands (solid lines) used to deconvolute the T−S and LD-(T−S) spectra (see also Table 1). Dashed lines represent the difference between the experimental spectra and the sum of the Gaussian bands.

TABLE 1: Simultaneous Gaussian Deconvolution of T−S and LD-(T−S) Spectra Using a Line Width of 80 cm^{-1} for All Bands[a]

ν [cm^{-1}]	λ [nm]	I_{T-S}	$I^{\lvert D\rvert-\lvert E\rvert}_{LD-(T-S)}$	$I^{\lvert D\rvert+\lvert E\rvert}_{LD-(T-S)}$	α_{T_y}	α_{T_x}
12 086	827.4	−1.00	−0.49	+0.32	6	83
12 269	815.1	+3.87	−1.05	+1.76	76	16
12 275	814.7	−3.99	+1.06	−1.68	76	21
12 411	805.8	−0.48	−0.18	+0.08	25	67
12 488	800.8	+0.07	+0.00	+0.02	≈55	≈75

[a] The deconvolution is obtained with a fitting routine using global analysis. The polarization of the bands with respect to the triplet axes, expressed by the angles α (in degrees), was calculated using eq 1.

to the triplet $\vec{x}_T\vec{y}_T$-plane. The Q_Y- and Q_X-transition dipole moments of the triplet-carrying molecule therefore lie both in the molecular plane spanned by its $\vec{x}_T$, $\vec{y}_T$ axes. This was also observed for monomer (B)Chls in frozen solution.[29] The bleaching of the 800 nm shoulder is too small to allow accurate determination of its polarization. The broad 795 nm band in the ground-state absorption spectrum (Figure 1) does not show up in the T−S spectrum, and at this point it is not possible to obtain the orientation of this transition moments with respect to the triplet axes.

We conclude that the T−S spectrum is dominated by only four different bands, a smaller number than would be expected on the basis of the number of pigments in the FMO-complex and the assumption of strong dipole−dipole interaction. Such an estimation *a priori* would predict either 7 different bands, assuming that the optical spectra are dominated by the interactions within a subunit only, or 21 different bands, if the interactions between the subunits within a trimer are included. Apparently only a few BChl molecules are effectively coupled to the triplet-carrying BChl. Considering that a constant value of R_i is observed for the long-wavelength band centered at 827 nm in the T−S spectrum and that this value is close to that observed for monomer BChl *a* in organic solvents, it seems unlikely that other BChls than the triplet-carrying molecule are involved in the corresponding transition.

3.2. The Effect of Dithionite. An EPR signal of an oxidized species has been observed in the FMO-complex of *Chlorobium tepidum*, which disappeared when dithionite was added.[37] This EPR signal was interpreted as arising from oxidized BChl *a*. In addition to this observation, it was reported that the absorption spectrum of the complex at 77 K was slightly altered upon addition of dithionite.[37] In contrast to those measurements, we find that the absorption spectrum at 1.2 K did not change after addition of dithionite. However, addition of dithionite seems to cause a splitting of the $|D| - |E|$ and $|D| + |E|$ transitions into 462 and 466 MHz and into 795 and 805 MHz, respectively as is shown in Figure 2. The maximum of the long-wavelength band in the T−S spectra varies slightly with the applied microwave frequency: the microwave transitions at lower frequencies (462 and 795 MHz) correspond to a maximum at 825−826 nm in the T−S spectra, whereas those at the higher frequencies correspond to a maximum at 827−828 nm. All other spectral features of the T−S spectra were identical to those obtained without addition of dithionite, irrespective of the microwave frequency. This indicates that addition of dithionite causes a slightly heterogeneous distribution of triplet states resulting in the observation of two conformations. We did not observe a characteristic signal of a radical in the EPR spectrum at 20 K of the antenna complex in the absence of dithionite as was reported in ref 37.

4. Discussion

4.1. Triplet State of the FMO-Complex. The zfs-parameters of the triplet state of the FMO-complex are very close to those of the triplet state of monomeric BChl *a* in organic solvents.[29,38] The small difference between the zfs-parameters of the FMO-complex and those observed for monomeric BChl *a* are typical for most antenna complexes, and can be attributed to differences in environment of the triplet-carrying molecule and to small changes of the charge-transfer and/or spin-orbit contributions to the properties of the triplet state.[39] The structure of the complex[4] shows that the intermolecular distances are too large for a significant overlap of molecular orbitals of the BChls and that the exchange interaction is too small to lead to triplet delocalization. Therefore, we conclude that the triplet state is localized on a single BChl *a* molecule. Note, that a distribution of the triplet state population over several chromophores would lead to a broadening of the ADMR line. The narrow line width and the well-defined zfs-parameters (see section Results) of the triplet state in the FMO-complex indicate, therefore, that the triplet state is always localized on the same chromophore in all subunits.

A negative sign of the ADMR signal, corresponding to an increase in ground-state absorption, has also been observed for other BChl *a* containing antenna systems,[40] but is opposite to that of BChl *a* in organic solvents.[29,30] The 9.5 GHz triplet EPR spectrum[41] of the FMO-complex shows a EEEAAA (A = enhanced absorption, E = stimulated emission) pattern, similar to that of BChl *a* in organic solvents. Such an EPR polarization pattern can only be explained by formation of the triplet state by intersystem crossing with population probabilities of the individual triplet sublevels p_x, $p_y >> p_z$. The ADMR signal depends on the total change in triplet population upon microwave irradiation, which in turn depends on population probabilities as well as decay kinetics of the triplet sublevels involved in the microwave transition.[42] In comparison to the positive ADMR sign of BChl *a* in organic solvents, the negative ADMR sign for the $|D| \pm |E|$ transitions in the FMO-complex can be

caused by slightly different populating probabilities and decay kinetics for the triplet *z*-sublevel compared to those of monomeric BChl *a* in organic solvents. For example, if the populating probability p_z of FMO is slightly higher than for monomeric BChl *a*, the ADMR sign will be reversed, while the decay rates might still be similar to those found for BChl *a*.[30,43] Such changes in population and decay kinetics might result from differences in the coordination of the central Mg atom, as observed for chlorophyll *a* in vesicles[44] or in the binding of the carbonyl groups.

The difference between the maximum at 825 nm in the absorption spectrum and the maximum at 827 nm in the T−S spectrum described in the Results section, could at first sight be related to a similar difference observed in monomeric BChl *a* in frozen solution.[29] The well-defined environment reflected by the narrow ADMR-line width in the FMO-complex, however, contrasts with the conformational variation for (B)Chls in frozen solution to which this difference was ascribed. In the accompanying paper, we will show that the optical steady-state spectra of the FMO-complex can be very well reproduced by an exciton simulation using only the seven BChls of a single subunit. We expect that, due to diagonal energetic disorder comparable to the inhomogeneous broadening, there is an average energy gap between the lowest excited states of the individual subunits of about 80 cm^{-1}. Consequently, relaxation within the manifold of excited states of an individual subunit is followed by energy transfer to the subunit of the FMO trimer that has the lowest excited state level. Most triplet states will be formed at this subunit, which thus contributes most to the long-wavelength bleaching in the T−S spectrum. We conclude therefore, that the difference between the maximum of the absorption and the T−S spectrum stems from (Förster-) energy transfer between the lowest excited states of the subunits within a trimeric FMO-complex. This conclusion is supported by the results of a study of the temperature dependence of optical dephasing times of the FMO-complex using accumulated photon echoes, which shows that energy transfer takes place between three electronic levels within the 825 nm absorption band.[45] Also, the negative polarization of the bleaching at wavelengths longer than 825 nm, which is observed upon excitation at 825 nm as described in ref 8, indicates that energy transfer takes place between two transitions with nearly perpendicular polarization.

4.2. Simulations of the T−S Spectra with Parameter Sets from the Literature. Simultaneous simulations of the absorption and CD-spectrum have been obtained by Pearlstein et al.[13,14] using an exciton model. While the results of the exciton calculations in the two papers were nearly identical, the use of equal line widths for corresponding transitions in the absorption- and CD-spectrum in ref 14 was a significant improvement of the parameter set in ref 13. In ref 14 the absorption and CD-spectra of Philipson and Sauer[10] and of Olson, Ke, and Thompson[11] were both simulated, however, with a different set of site energies. For both simulations, line widths varying between 95 and 340 cm^{-1} were assigned to the individual transitions. These line widths were optimized to fit the experimental spectra and do not exhibit a trend such as an increase towards short wavelengths, which might be expected if lifetime broadening is significant.

The exciton calculations for the FMO-trimer of Pearlstein et al.[13,14] use the full Hamiltonian, with 21 BChls with equal site energies for corresponding BChls in different subunits of the trimer, leading to 14 degenerate and 7 nondegenerate eigenstates. Inclusion of all 21 BChls was necessary for fitting the CD-spectrum,[13] which seemed to be impossible using the interactions

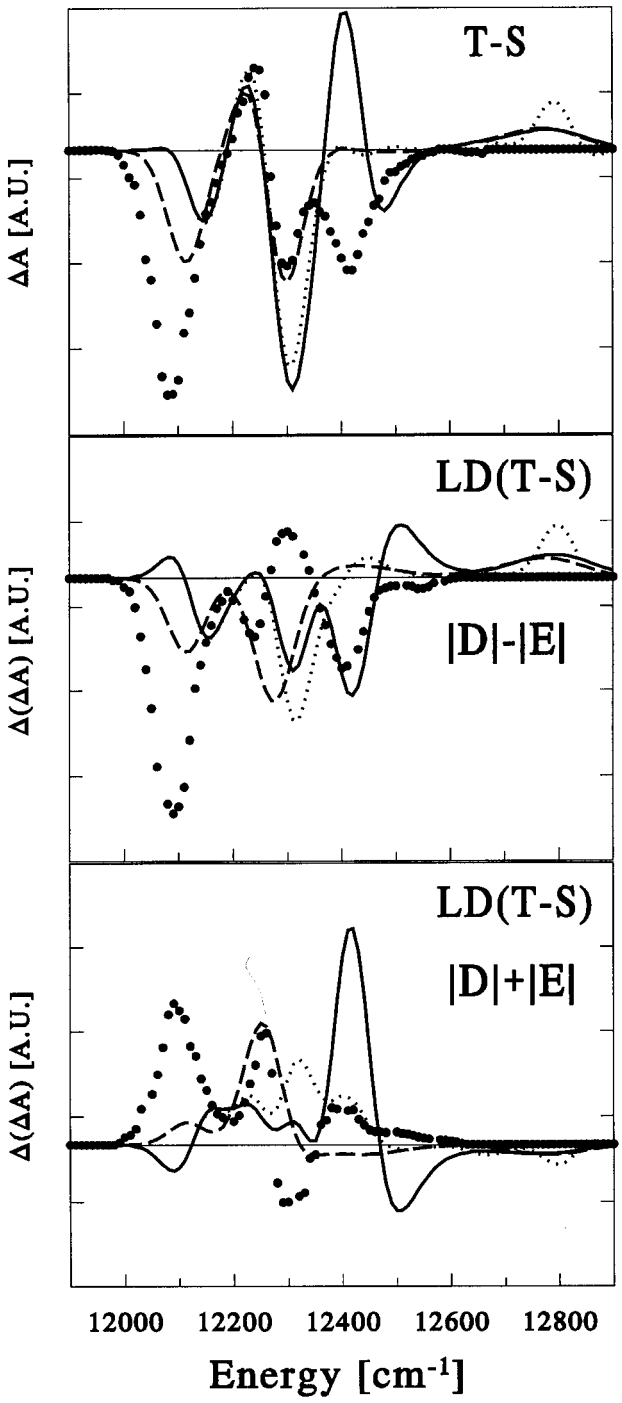

Figure 6. Exciton simulation (solid lines) of T−S and LD-(T−S) spectra (solid circles) with parameter set taken from ref 13. In this set of parameters, the dipolar interaction energies are calculated within the point-monopole approximation and 21 BChls are used. Broken lines represent simulations with a Hamiltonian including the seven BChls of a single subunit only. Dotted lines represent simulations using the 21 BChls of the original parameter set again, but the line widths are replaced by 80 cm^{-1}. The vertical scales used for the LD-(T−S) spectra are enlarged by a factor of 2 compared to the vertical scale used for the T−S spectrum.

between the 7 BChls in a single subunit. Similarly, the exciton simulations of the LD- and the T−S-spectrum by Gülen[19] are based on the full Hamiltonian with 21 BChls. In this section we present exciton simulations of our LD-(ADMR) data using two representative parameter sets taken from refs 13, 14, and 19. The results of these simulations are plotted in Figure 6 for the parameter set used in ref 13 to simulate the absorption- and CD-spectrum and in Figure 7 for the parameter set used by

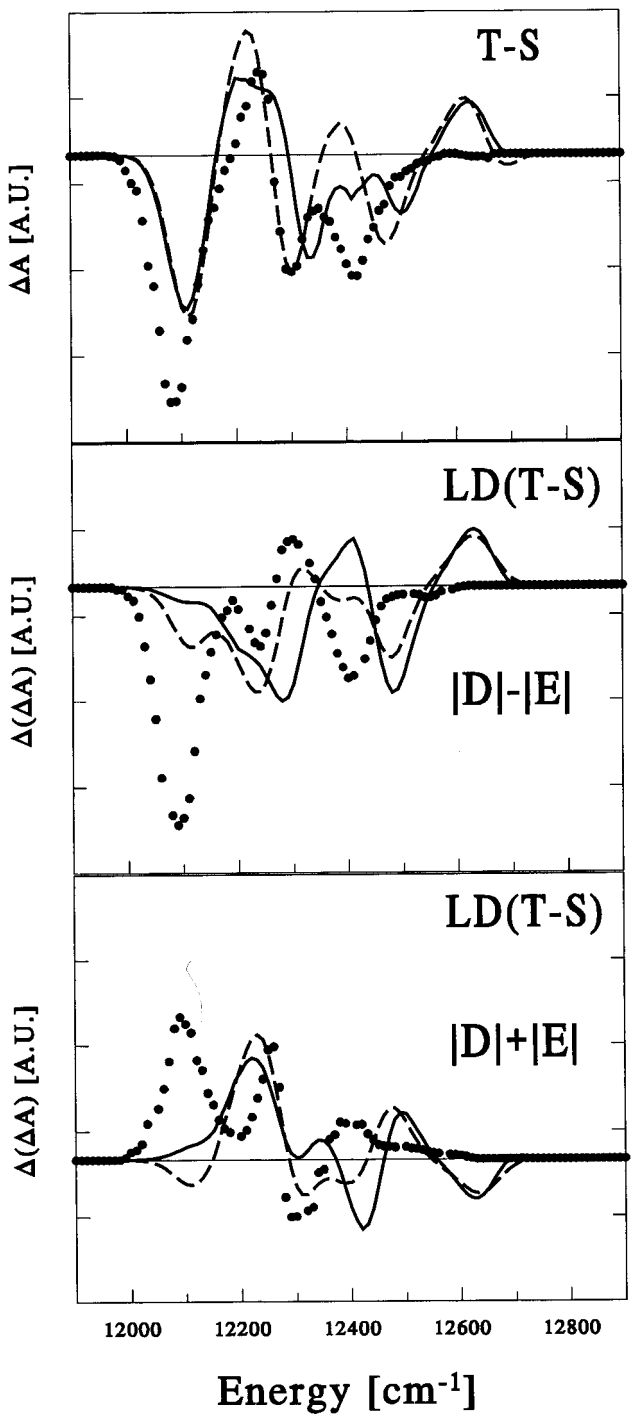

Figure 7. Exciton simulations with the parameter set taken from Gülen.[19] Scales, lines, and markers as in Figure 6.

Gülen[19] to simulate the absorption-, LD- and flash-induced T−S spectrum from ref 8. As mentioned above, these parameter sets use a full Hamiltonian of 21 sites and, except for the latter, use unequal line widths for the various transitions. To facilitate comparison with the simulations we will present in the accompanying paper, we also include simulations which use an equal line width for all transitions, as well as simulations using a Hamiltonian of only 7 sites. The LD-(T−S) were simulated including a small difference in site energy between the corresponding sites of the different subunits (see the accompanying article).

At first sight, the parameter set of Gülen seems to improve the simulation of the T−S spectrum considerably compared to the simulations using the parameter sets of Pearlstein et al. A critical inspection, however, shows that there still exist large discrepancies between the experimental and simulated spectra. As described above, the polarization of the 827 nm band in the experimental T−S spectrum approaches the monomer polarization of an isolated BChl, and there is no evidence that the bleaching at 827 nm is accompanied by another band, demonstrating that the contribution of the triplet-carrying molecule to the lowest excited state exceeds by far those of the other BChls. In contrast to these experimental observations, in the exciton simulations with the parameter sets from Pearlstein and Gülen, there are three excited states in the 827 nm region. These excited states are delocalized predominantly over BChls 6 and BChls 7, and BChls 5 and 6, respectively. This delocalization results in a polarization of the bleaching upon triplet formation at the longest wavelengths that differs significantly from the polarization of the transition dipole moment of the triplet-carrying molecule, and in an induced absorption at the short wavelength side of this bleaching. Furthermore, the bandshift around 815 nm in the experimental T−S spectrum, seems not to be accompanied by a change in polarization, while the excited states absorbing around 800 and 805 nm predominantly display a loss of dipole strength, and do not show a significant shift in energy upon triplet formation, in contrast to the simulations presented in Figures 6 and 7.

We note that, in the simulations using the parameter sets of refs 13 and 14, a large reorganization of dipole strength takes place upon triplet formation, even at wavelengths below 795 nm. In both simulations this is due to a rather strong (relative to the difference in site energy) dipolar interaction between the triplet-carrying molecules (BChl 6 in ref 19 and BChl 7 in ref 13) and their neighbors, resulting in largely delocalized states.

We thus surmise that the deviations between the simulated and experimental spectra presented here are mainly caused by an overestimation of the dipolar interaction between the chromophores of the complex. In other words, the Q_Y absorption region in the various optical spectra seems to be characterized rather by differences in site energy of the individual BChls than by the dipolar interaction between them. In the accompanying paper we explore these ideas further and show that reducing the dipolar interactions indeed leads to an acceptable fit of *all* available experimental spectra.

5. Conclusions

ADMR spectroscopy shows that the triplet state of the FMO-complex of the green sulfur bacterium *P. aestuarii* exhibits identical zfs-parameters as those of BChl *a* in organic solvents. It follows that the triplet state of this complex is localized on a single BChl. The remarkably small line width of the ADMR-transition indicates that this BChl is the same for all complexes.

The T−S and the LD-(T−S) spectra are very similar, apart from a different sign for the various bands. With global analysis it is demonstrated that these spectra can be fitted to a sum of a limited number of Gaussian bands. We find that three Gaussians account for the bleachings at 800, 805, and 827 nm, and a combination of a negative and a positive Gaussian band accounts for the bandshift around 814/815 nm.

The orientation of the optical transition dipole corresponding to the 827 nm band with respect to the triplet *y*- and *x*-axis is found to be more or less parallel and perpendicular to these triplet axes, respectively, similar to what has been observed for monomer BChl in various organic solvents. The polarizations of the 805 nm band and the 815 nm bands are parallel and perpendicular to the 827 nm transition dipole moment, respectively, all with transition dipole moments approximately polarized in the triplet $\vec{x}_T\vec{y}_T$-plane of the triplet-carrying BChl. The

amplitudes of the 800 nm band in the various spectra are too small to allow accurate determination of the orientation of the corresponding transition dipole moment.

Exciton simulations of the T−S and LD-(T−S) spectra using parameter sets from the literature deviate substantially from the experimental spectra. In the accompanying paper we will present a parameter set that significantly improves the match between the simulated and experimental spectra, including the absorption-, LD-, CD-, (T−S)-, and LD-(T−S) spectra of the FMO-complex.

Acknowledgment. We thank Christof Francke for his support in isolating the FMO-complex. This investigation was supported by the Life Science Foundation (SLW) and the Foundation for Chemical Research (SON), financed by the Netherlands Organization for Scientific Research (NWO), and by the European Community (Contract FMRX-CT96-0081). We are indebted to Prof. J. Amesz for critically reading the manuscript.

References and Notes

(1) Olson, J. M. In *The Chlorophylls*; Vernon, L. P., Seeley, G. R., Eds.; Academic Press: New York, **1966**; p 413.
(2) Fenna, R. E.; Matthews, B. W.; Olson, J. M.; Shaw, E. K. *J. Mol. Biol.* **1974**, *84*, 231.
(3) Matthews, B. W.; Fenna, R. E. *Acc. Chem. Res.* **1980**, *13*, 309.
(4) Tronrud, D. E.; Schmidt, M. F.; Matthews, B. W. *J. Mol. Biol.* **1986**, *188*, 443.
(5) Olson, J. M. In *The Photosynthetic Bacteria*; Clayton, R. K., Sistrom, W. R., Eds.; Plenum Press: New York, **1978**; p 161.
(6) Whitten, W.; Pearlstein, R. M.; Phares, E. F.; Geacintov, N. E. *Biochim. Biophys. Acta* **1978**, *503*, 491.
(7) Swarthoff, T.; de Grooth, B. G.; Meiburg, R. F.; Rijgersberg, C. P.; Amesz, J. *Biochim. Biophys. Acta* **1980**, *593*, 51.
(8) van Mourik, F.; Verwijst, R. R.; Mulder, J. M.; van Grondelle, R. *J. Phys. Chem.* **1994**, *98*, 10307.
(9) Vasmel, H.; Swarthoff, T.; Kramer, H. J. M.; Amesz, J. *Biochim. Biophys. Acta* **1983**, *725*, 361.
(10) Philipson, K. D.; Sauer, K. *Biochemistry* **1972**, *11*, 1880.
(11) Olson, J. M.; Ke, B.; Thompson, K. H. *Biochim. Biophys. Acta* **1976**, *430*, 524.
(12) Francke, C.; Amesz, J. *Photosynth. Res.* **1997**, *52*, 137.
(13) Pearlstein, R. M. *Photosynth. Res.* **1992**, *31*, 213.
(14) Lu, X.; Pearlstein, R. M. *Photochem. Photobiol.* **1993**, *57*, 86.
(15) Gulbinas, V.; Valkunas, L.; Kuciauskas, D.; Liuolia, A.; Katilius, E.; Zhou, W.; Blankenship, R. E. *J. Phys. Chem.* **1996**, *100*, 17950.
(16) Savikhin, S.; Struve, W. S. *Photosynth. Res.* **1996**, *48*, 271.
(17) Buck, D. E.; Savikhin, S.; Struve, W. S. *Biophys. J.* **1997**, *72*, 24.
(18) Johnson, S. G.; Small, G. J. *J. Phys. Chem.* **1991**, *95*, 471.
(19) Gülen, D. *J. Phys. Chem.* **1996**, *100*, 17683.
(20) Vrieze, J.; Hoff, A. J. *Biochim. Biophys. Acta* **1996**, *1276*, 210.
(21) den Blanken, H. J.; Meiburg, R. F.; Hoff, A. J. *Chem. Phys. Lett.* **1984**, *105*, 336.
(22) Meiburg, R. F. Ph.D. Thesis, University of Leiden, The Netherlands, 1985.
(23) Verméglio, A.; Breton, J.; Paillotin, G.; Cogdell, R. *Biochim. Biophys. Acta* **1978**, *501*, 514.
(24) Miller, M.; Cox, R. P.; Olson, J. M. *Photosynth. Res.* **1994**, *41*, 97.
(25) den Blanken, H. J.; Hoff, A. J. *Biochim. Biophys. Acta* **1982**, *681*, 365.
(26) Dunlap, D. A.; Samori, B.; Bustamante, C. In *Polarised Spectroscopy of Ordered Systems*; Samori, B., Thulstrup, E. W., Eds.; Kluwer Academic Publishers: Dordrecht, 1988; p 275.
(27) Louwe, R. J. W.; Vrieze, J.; van der Vos, R.; Aartsma, T. J.; Hoff, A. J. In preparation.
(28) Pearlstein, R. M. In *Chlorophylls*; Scheer, H., Ed.; CRC Press: Boca Raton, 1991; p 1047.
(29) Vrieze, J.; Hoff, A. J. *Chem. Phys. Lett.* **1995**, *237*, 493.
(30) den Blanken, H. J.; Meiburg, R. F.; Hoff, A. J. *Chem. Phys. Lett.* **1983**, *96*, 343.
(31) Vasmel, H.; den Blanken, H. J.; Dijkman, T.; Hoff, A. J.; Amesz, J. *Biochim. Biophys. Acta* **1984**, *767*, 200.
(32) Angerhofer, A.; von Schütz, J. U.; Wolf, H. C. *Z. Natürforsch.* **1984**, *C39*, 1085.
(33) den Blanken, H. J.; Jongenelis, A. P. J. M.; Hoff, A. J. *Biochim. Biophys. Acta* **1983**, *725*, 472.
(34) Owen, G. M.; Jones, M. R.; Hoff, A. J. *J. Phys. Chem.* B **1997**, *101*, 7197.
(35) Petke, J. D.; Maggiora, G. M.; Shipman, L.; Christoffersen, R. E. *Photochem. Photobiol.* **1979**, *30*, 203.
(36) Petke, J. D.; Maggiora, G. M.; Shipman, L.; Christoffersen, R. E. *Photochem. Photobiol.* **1980**, *32*, 399.
(37) Zhou, W.; LoBrutto, R.; Lin, S.; Blankenship, R. E. *Photosynth. Res.* **1994**, *41*, 89.
(38) Angerhofer, P. O. J. In *Chlorophylls*; Scheer, H., Ed.; CRC Press: Boca Raton, 1991; p 945.
(39) Beese, D.; Steiner, R.; Scheer, H.; Angerhofer, A.; Robert, B.; Lutz, M. *Photochem. Photobiol.* **1988**, *47*, 293.
(40) Jirsikova, V.; Reisshusson; Agaldis; Vrieze, J.; Hoff, A. J. *Biochim. Biophys. Acta* **1995**, *1231*, 313.
(41) Louwe, R. J. W.; Hulsebosch, B.; Vrieze, J.; Gast, P.; Aartsma, T. J.; Hoff, A. J. Article in preparation.
(42) Hoff, A. J. In *Advanced EPR. Applications in Biology and Biochemistry*; Hoff, A. J., Ed.; Elsevier: Amsterdam, **1989**; p 633.
(43) Clarke, R. H.; Conners, R. E.; Frank, H. A.; Hoch, J. C. *Chem. Phys. Lett.* **1977**, *45*, 523.
(44) Fragata, M.; Nórden, B.; Kuruscev, T. *Photochem. Photobiol.* **1988**, *47*, 133.
(45) Louwe, R. J. W.; Aartsma, T. J. *J. Phys. Chem.* B **1997**, *101*, 7221.